nature chemical biology

Article

https://doi.org/10.1038/s41589-023-01534-9

Fast and sensitive CRISPR detection by minimized interference of target amplification

Received: 20 March 2023

Accepted: 19 December 2023

Published online: 08 February 2024

Check for updates

Xiaohan Tong[1,2,8], Kun Zhang[1,2,8], Yang Han[3,8], Tianle Li[1,2], Min Duan[1,2], Ruijin Ji[1,2], Xianguang Wang[3], Xi Zhou[4], Ying Zhang[1,5] & Hao Yin[1,2,6,7]

Despite the great potential of CRISPR-based detection, it has not been competitive with other market diagnostics for on-site and in-home testing. Here we dissect the rate-limiting factors that undermine the performance of Cas12b- and Cas13a-mediated detection. In one-pot testing, Cas12b interferes with loop-mediated isothermal amplification by binding to and cleaving the amplicon, while Cas13a directly degrades the viral RNA, reducing its amplification. We found that the protospacer-adjacent motif-interacting domain engineered Cas12b accelerated one-pot testing with 10–10,000-fold improved sensitivity, and detected 85 out of 85 SARS-CoV-2 clinical samples with a sensitivity of 0.5 cp μl^{-1}, making it superior to wild-type Cas12b. In parallel, by diminishing the interference of Cas13a with viral RNA, the optimized Cas13a-based assay detected 86 out of 87 SARS-CoV-2 clinical samples at room temperature in 30 min with a sensitivity of 0.5 cp μl^{-1}. The relaxed reaction conditions and improved performance of CRISPR-based assays make them competitive for widespread use in pathogen detection.

The outbreak of infectious diseases has resulted in substantial morbidity and mortality, as well as social and economic disruption[1–7]. The coronavirus disease 2019 (COVID-19) pandemic has led to at least 6 million deaths and over 600 million infections worldwide[8–10]. Surveillance systems play a crucial role in mitigating disease transmission, although the centralized diagnostic laboratory model has its limitations[11]. Quantitative polymerase chain reaction (qPCR), the primary test used in laboratories, demands skilled operators and expensive infrastructure[12–15]. Additionally, the sample-to-answer time for qPCR typically ranges from 4 to 24 h (refs. 12–15). Aspects such as sample transportation and data reporting can also contribute to the overall turnaround time of centralized molecular testing. Developing a point-of-care detection method that is sensitive, rapid, straightforward and cost-effective could facilitate early detection, an imperative factor in controlling disease transmission.

The antigen test has found widespread use at home for diagnosing severe acute respiratory syndrome coronavirus 2 (SARS-CoV-2) infections. This kind of point-of-care kit is cost-effective and rapid, producing results within 15–30 min at room temperature[16–19]. Nevertheless, its sensitivity falls markedly short of that of qPCR, resulting in a relatively elevated false-negative rate[18,19]. Point-of-care nucleic acid detection assays using isothermal amplification methods such as recombinase

[1]Department of Clinical Laboratory, Frontier Science Center for Immunology and Metabolism, Medical Research Institute, Zhongnan Hospital of Wuhan University, Wuhan University, Wuhan, China. [2]State Key Laboratory of Virology, TaiKang Centre for Life and Medical Sciences, TaiKang Medical School, Wuhan University, Wuhan, China. [3]Center for Translational Medicine, Wuhan Jinyintan Hospital, Wuhan, China. [4]State Key Laboratory of Virology, Wuhan Institute of Virology, Chinese Academy of Sciences, Wuhan, China. [5]Department of Rheumatology and Immunology, Zhongnan Hospital of Wuhan University, Wuhan University, Wuhan, China. [6]Department of Urology, Frontier Science Center for Immunology and Metabolism, Medical Research Institute, Zhongnan Hospital of Wuhan University, Wuhan University, Wuhan, China. [7]Wuhan Research Center for Infectious Diseases and Cancer, Chinese Academy of Medical Sciences, Wuhan, China. [8]These authors contributed equally: Xiaohan Tong, Kun Zhang, Yang Han. e-mail: haoyin@whu.edu.cn

polymerase amplification (RPA) and loop-mediated isothermal amplification (LAMP) exhibit higher sensitivity than the antigen test. However, they often come with substantial false-positive rates[20–23].

The CRISPR–Cas (clustered regularly interspaced short palindromic repeats-CRISPR-associated proteins) system has been adopted in various applications, including recently developed pathogen detection[24–28]. On recognition of nucleic acid sequences through guide RNA (gRNA), Cas13 or Cas12 nucleases exhibit nonspecific nuclease activity, cleaving single-stranded (ss) RNA or ssDNA, respectively, a phenomenon known as *trans*-cleavage[29–34]. The *trans*-cleavage of a caged reporter molecule generates signals that can be detected by a fluorescence reader[29–34]. Despite the high specificity of CRISPR, it takes hours for Cas13 nucleases alone to reach attomolar sensitivity[32,33,35]. Using unrelated CRISPR nucleases in tandem can expedite RNA detection, but its sensitivity remains lower than that of isothermal amplification or PCR[26]. Consequently, viral samples undergo isothermal amplification and the resultant amplicon can then be used for CRISPR-based detection[29,36–43]. Cas12-based DNA endonuclease-targeted CRISPR *trans* reporter (DETECTR) and Cas13-based specific high sensitivity enzymatic reporter unlocking (SHERLOCK) bifurcate the amplification and detection into two distinct steps, resulting in substantially enhanced sensitivity compared to using only Cas12 or Cas13. However, the incorporation of multiple steps leads to increased complexity, extended reaction time, and an elevated risk of cross-contamination[29,36,38,39]. Isothermal amplification and CRISPR detection were subsequently integrated into a single step, leading to the creation of methods such as SHINE (streamlined highlighting of infections to navigate epidemics) and STOPCovid (specific high sensitivity enzymatic reporter unlocking testing in one pot)[40,41,44]. SHINEv2 improved on SHINE by consolidating multiple heating steps into a single 90-min heating phase and eliminating the necessity for cold temperature storage of the reagents[44]. Despite their straightforward operational process and reduced risk of cross-contamination, the sensitivities of one-pot testing methods are often lower than those of two-step approaches. Additionally, these one-pot tests often require a longer reaction time[40,41]. It is of great need to develop a robust, rapid and uncomplicated CRISPR-based detection method for on-site testing.

Isothermal amplification assays compatible with a portable device are popular in clinics for rapid testing. A well-developed isothermal amplification assay using LAMP for detecting the influenza virus can achieve a sensitivity of approximately 4 cp μl^{-1} within 30 min, along with an approximately 10% false-positive rate[45,46]. By contrast, the recently developed CRISPR detection assays STOPCovid and DISCoVER attain sensitivities of approximately 10 or 40 cp μl^{-1} within 40 min (refs. 41,43). Despite the high specificity of CRISPR-based detection, these assays have not demonstrated notable advantages over isothermal amplification assays. For in-home testing, antigen test kits are widely used. While the sensitivity of most CRISPR-based detection methods greatly surpasses that of antigen test kits, the substantial cost associated with CRISPR-based detection hinders its widespread adoption. A key cost factor for CRISPR-based assays is the requirement for customers to purchase temperature-control equipment for in-homing testing. By contrast, antigen test kits can be conducted at room temperature[16–19].

In this study, we explored the factors constraining the performance of Cas12b- and Cas13a-mediated nucleic acid detection. Both Cas12b and Cas13a compromised the amplification of target sequences, resulting in reduced sensitivity and speed of one-pot testing. We identified a universal approach through protein engineering of protospacer-adjacent motif (PAM)-interacting domains to enhance the performance of one-pot testing for Cas12 orthologs. The engineered Cas12b mutant demonstrated the capability to detect SARS-CoV-2 at levels as low as 0.5 cp μl^{-1} within 15 min, and its performance is much superior than STOPCovid. Furthermore, our investigation revealed that Cas13a directly degraded viral RNA in SHINE. By devising an amplification process that strategically avoids such degradation, we notably improved the efficacy of viral RNA detection. This advancement enabled the detection of SARS-CoV-2 samples in just 30 min at room temperature (20 °C), yielding sensitivity levels comparable to those of qPCR with reverse transcription (RT–qPCR). These assays developed in our study fulfill the inherent potential of CRISPR-based detection, presenting substantial advantages over other widely used tools for rapid detection.

Results

One-pot testing using suboptimal PAMs of Cas12b

In a previous study, we discovered that in one-pot testing Cas12a cleavage could interfere with isothermal amplification, and by tuning the kinetics of cleavage through suboptimal PAM for Cas12a could greatly enhance the sensitivity and reproducibility of the detection[42]. To determine whether this suboptimal PAM approach could be extended to other Cas12 orthologs for one-pot testing, we compared the performance of canonical PAM sequences and suboptimal PAMs for AapCas12b. We evaluated 18 suboptimal PAMs using three spacers targeting the *N* gene of SARS-CoV-2. Unlike the outcomes observed with Cas12a, the fluorescence curves obtained from spacers using suboptimal PAMs for AapCas12b did not demonstrate superior performance compared to those using canonical PAMs. This was the case regardless of whether LAMP or RPA was used as the isothermal amplification method (Extended Data Fig. 1a–f). We speculated that adjusting the PAM sequence for AapCas12b (TTN) might not be as adaptable as it is for LbCas12a (TTTV), and even a single nucleotide mutation within AapCas12b's PAM could severely impair its activity.

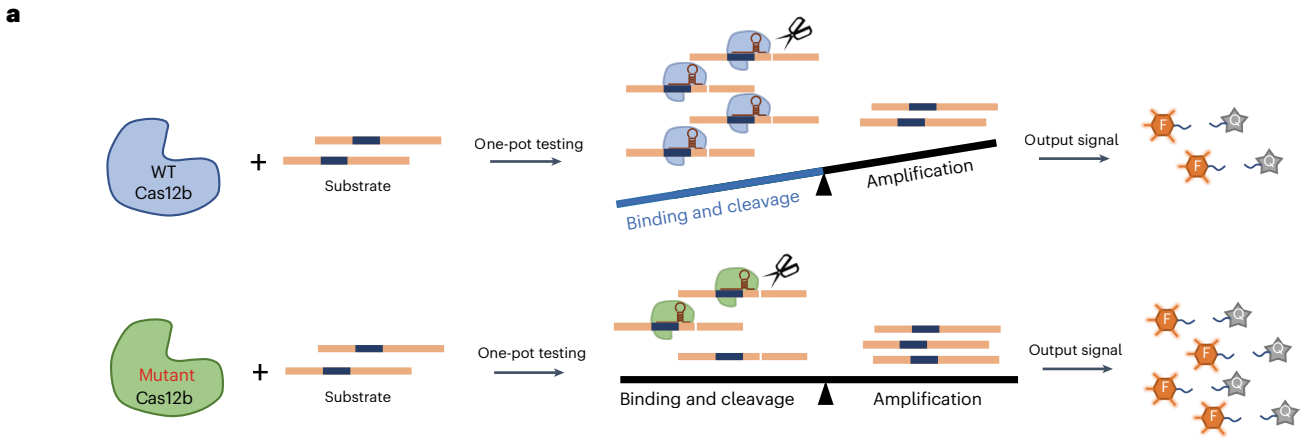
Structure-guided Cas12b mutations for one-pot testing

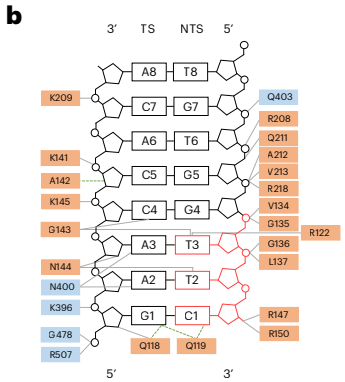
We hypothesized that by substituting residues within the PAM-interacting domain of Cas12b, we could tune its activity to improve one-pot testing. To enhance the sensitivity and speed of Cas12b-mediated CRISPR detection, we used a known AacCas12b-single-guide (sg) RNA-dsDNA ternary structure as a guide for engineering AapCas12b, given their substantial conservation (Fig. 1a,b)[47]. AapCas12b's amino acids that have hydrogen bonds with the substrates were mutated to alanine, and mutants that outperformed the wild-type (WT) were selected based on their performance in LAMP-mediated one-pot testing (Fig. 1c,d and Extended Data Fig. 2). Among the mutants that exhibited stronger fluorescent signals than the WT, a common G478A mutation was identified and a mutant with double mutations G478A/K396A generated the strongest signal

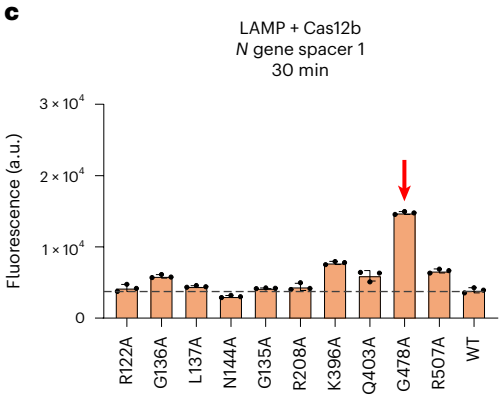
Fig. 1 | Mutants of AapCas12b enable faster and more sensitive one-pot testing than WT. a, Schematic depiction of the isothermal amplification and cleavage process in AapCas12b-WT and AapCas12b mutant-mediated one-pot testing. F and Q indicate fluorophore and quencher, respectively. **b**, Illustration of residues interacting with PAM and DNA in AacCas12b. The structure of AapCas12b is highly conserved with AacCas12b. **c**,**d**, Fluorescence profiles of AapCas12b-WT and mutants in LAMP-mediated one step testing. Single mutation (**c**) and double mutations (**d**) were tested using *N* gene spacer 1. The red arrows point to AapCas12b mutant G478A and G478A/K396A (AapCas12b-2M, 2M indicates double-point mutations). For *N* gene spacer 1, 20 fg dsDNA substrates was used. **e**–**g**, Fluorescence signals of WT and AapCas12b-2M using *N* gene spacer 1 (**e**), spacer 2 (**f**) or spacer 3 (**g**) in LAMP-mediated one-pot testing. The fluorescence values were determined using a qPCR instrument. The substrates for *N* gene spacer 1, 2, 3 were 20, 2,000 and 2 fg dsDNA, respectively. NC indicates the negative control. **h**–**j**, Comparison of sensitivity in one-pot testing using WT or AapCas12b-2M. Fluorescence values were determined using the SpectraMax i3x. The dsDNA substrates were *N* gene spacer 1 (**h**), spacer 2 (**i**) and spacer 3 (**j**). The black dashed lines signify the threshold value, defined as three times the value of the negative controls. Mean ± s.d. of $n = 3$ technical replicates for **c**–**j**. a.u., arbitrary units.

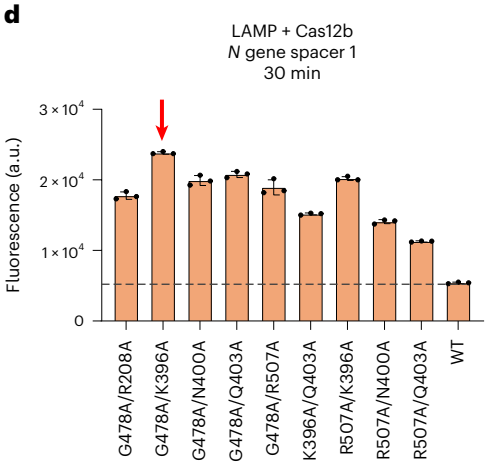
https://doi.org/10.1038/s41589-023-01534-9

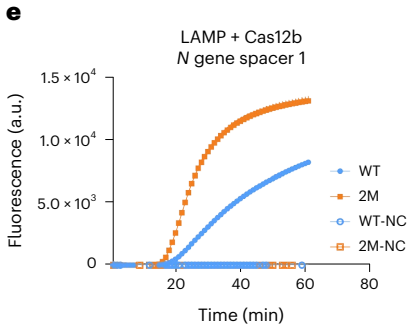
(Fig. 1c,d and Extended Data Fig. 2). We designated this modified Aap-Cas12b as 'Cas12b-2M' and evaluated its performance using various spacers in LAMP-mediated one-pot testing. Across all three tested spacers, Cas12b-2M displayed accelerated kinetics compared to the WT (Fig. 1e–g), resulting in a sensitivity improvement ranging from 10- to 10,000-fold, along with a substantially enhanced signal-to-noise ratio (Fig. 1h–j). Notably, glycine 478 is conserved within the Cas12b family across multiple species, and lysine 396 exhibits conservation between

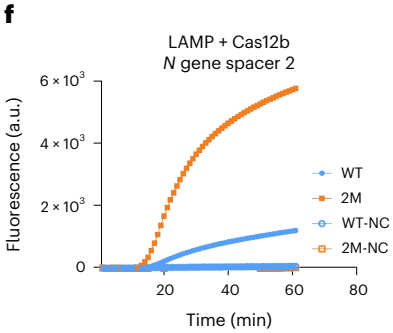


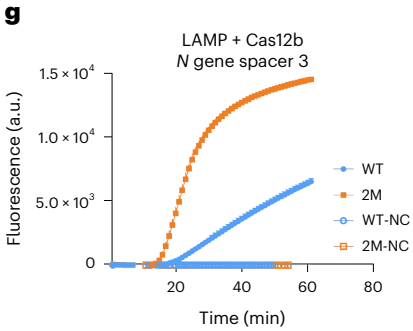


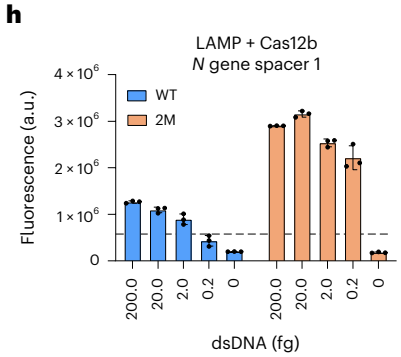


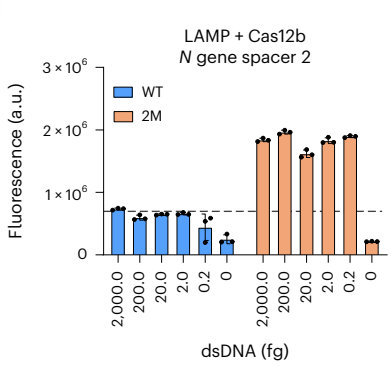


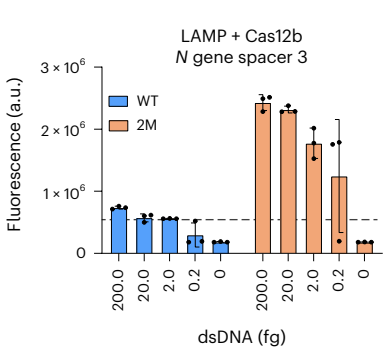












https://doi.org/10.1038/s41589-023-01534-9

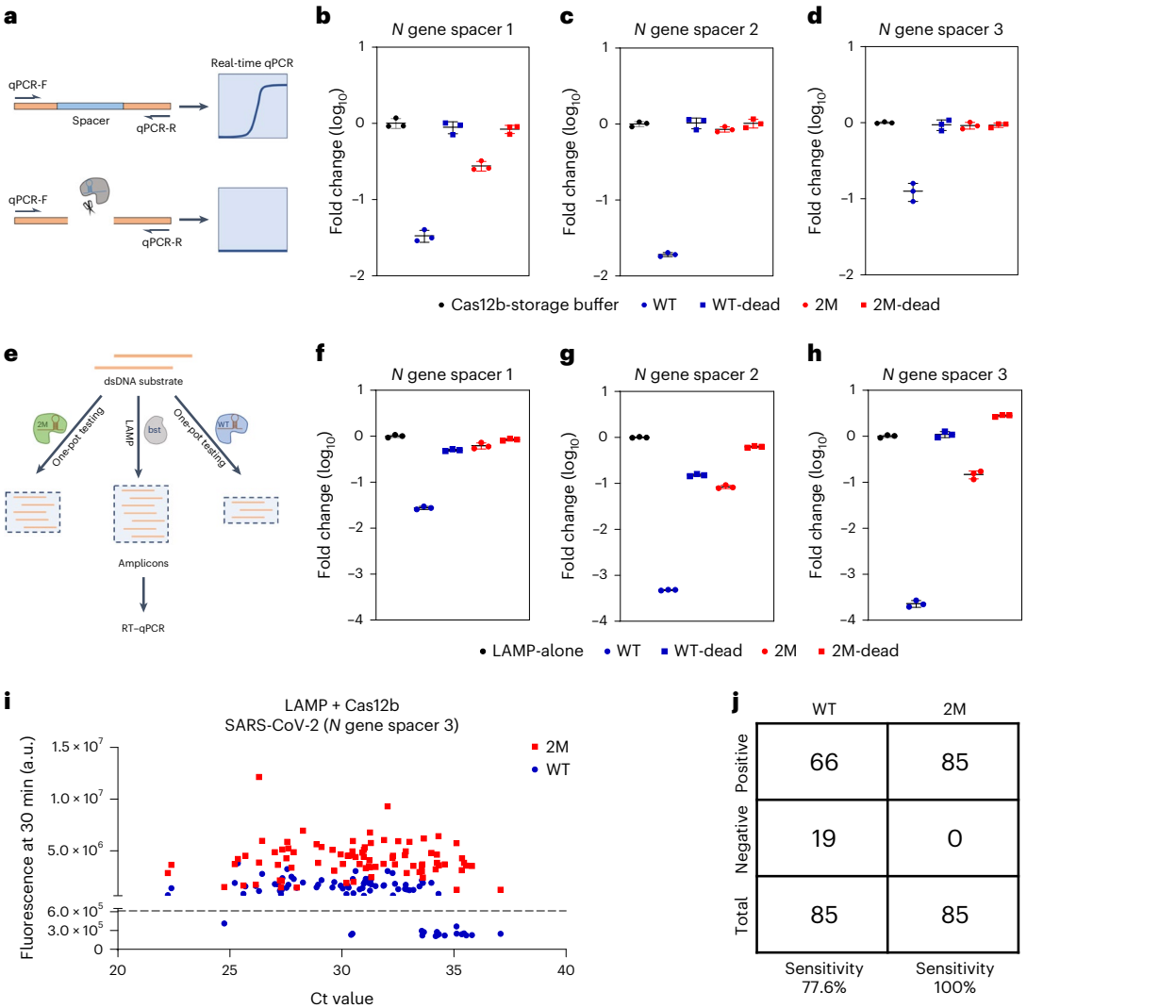


Fig. 2 | Detection of SARS-CoV-2 clinical samples using the AapCas12b mutant. a, Schematic diagram to illustrate the assay to determine *cis*-cleavage activity. **b**–**d**, Quantification of *cis*-cleavage using qPCR. The remaining substrates in AapCas12b-WT and AapCas12b-2M after 1 min of incubation at 60 °C were quantified using qPCR. The dsDNA substrates of *N* gene spacer 1 (**b**), spacer 3 (**c**) and spacer 3 (**d**) were used. Amplicon levels were normalized to the substrate levels in the Cas12b-storage buffer group. **e**, Schematic diagram to illustrate the assay for quantifying amplicons. bst indicates *Bacillus stearothermophilus* DNA polymerase. **f**–**h**, Quantification of amplicons in one-pot testing using qPCR. One-pot testing samples were incubated at 60 °C for 8 min, and 2 µl of diluted products was introduced into the qPCR reaction. The dsDNA substrates were *N* gene spacer 1 (**f**), spacer 2 (**g**) and spacer 3 (**h**). Amplicon levels were normalized to those in the LAMP alone group. Mean ± s.d. of $n = 3$ technical replicates for **b**–**d** and **f**–**h**. **i**, One-pot testing using AapCas12b-2M or WT to detect 85 positive SARS-CoV-2 nasopharyngeal swab samples was conducted at 61 °C in 30 min. Fluorescence values were measured using SpectraMax i3x. The sgRNA targeting *N* gene spacer 3 was used. The black dashed line represents the threshold, set at three times the negative control fluorescence values. **j**, Concordance analysis of **i**.

AapCas12b and AacCas12b, suggesting that these mutations could potentially be applied to other Cas12b orthologs (Extended Data Fig. 2).

To explore how Cas12-2M improved one-pot testing, we conducted a comparison of the cleavage activities between Cas12b-WT and Cas12b-2M. As controls, an enzymatically dead Cas12b-WT and a dead Cas12b-2M were engineered and expressed, and their *cis*-cleavage activities were verified to be eliminated (Extended Data Figs. 2 and 3 and Fig. 2a–d). Quantification of the uncleaved substrate through qPCR was carried out after 1 min of incubation with Cas12b. Notably, within this 1-min period, the uncleaved products in Cas12b-2M-treated samples exhibited 7.4–44.4 times greater quantity compared to Cas12b-WT-treated samples, suggesting Cas12b-2M exerts reduced interference on the initial step of isothermal amplification (Fig. 2a–d). Furthermore, we quantified the amplicons generated during a one-pot testing. The Cas12b-2M group displayed an average of a 6.8-fold reduction in amplicon quantity compared to LAMP alone, while the Cas12b-WT group exhibited a substantial decrease with amplicon quantities ranging from 46 to 4,420-fold fewer than in the LAMP alone (Fig. 2e–h). This observation indicates that Cas12b-2M substantially reduced interference with the LAMP process. The enzymatically dead Cas12b-WT displayed a minor effect on hindering amplification, likely stemming from its ability to bind to the substrate and impede the amplification process. This hindering effect was further diminished in the case of the enzymatically dead Cas12b-2M group (Fig. 2f–h).

Detection of SARS-CoV-2 samples using Cas12b-2M

To further enhance the efficiency of one-pot testing, we screened several commercially available Bst DNA polymerase, the solo enzyme used in the LAMP reaction. Cas12b-2M, in conjunction with the optimal polymerase selection, detected pseudo-SARS-CoV-2 RNA within 15 min with a limit of detection (LOD) as low as 0.5 cp μl^{-1} (Extended Data Fig. 4a,b). In the assessment of SARS-CoV-2 clinical samples, Cas12b-2M detected

https://doi.org/10.1038/s41589-023-01534-9

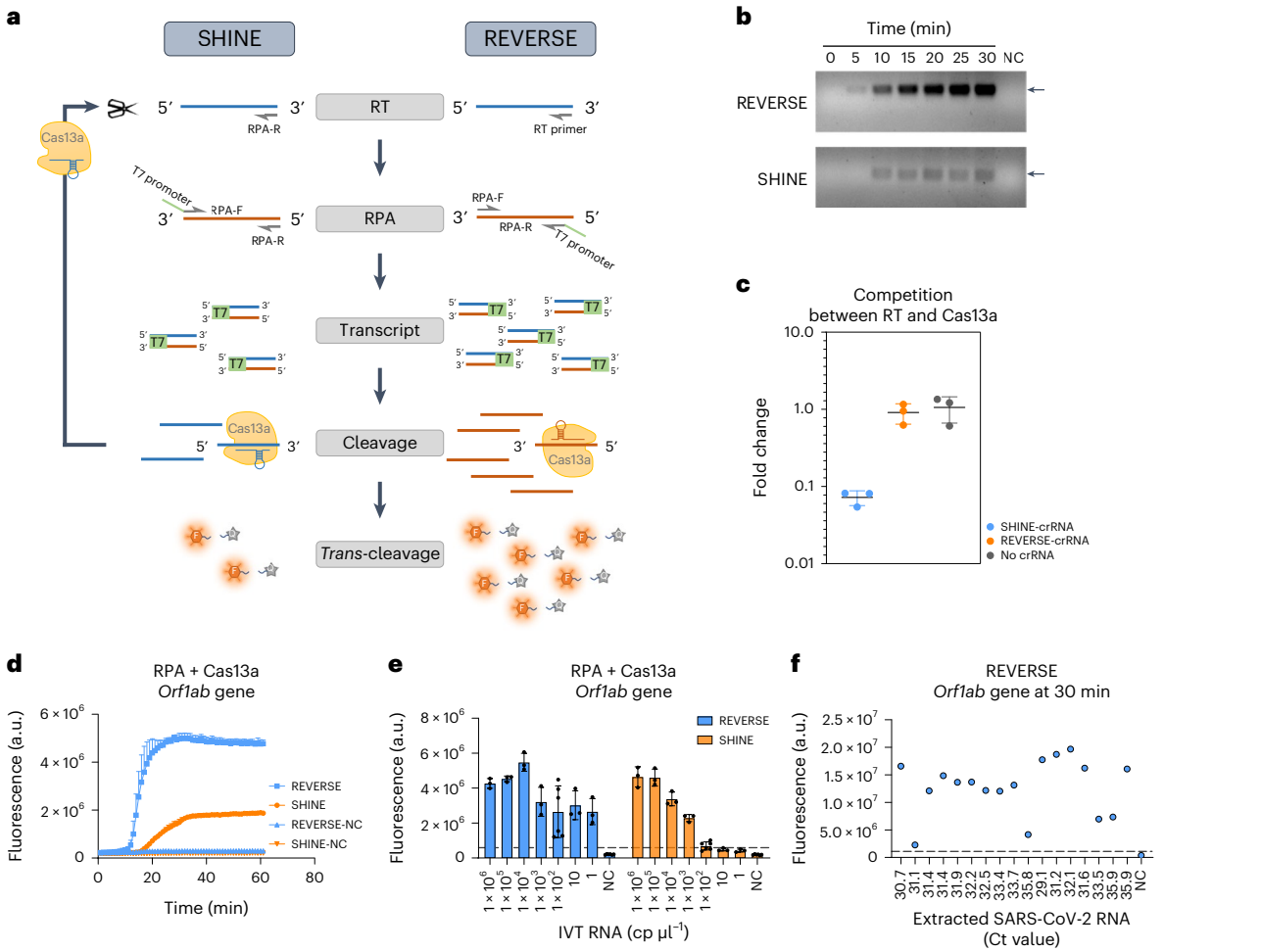


Fig. 3 | REVERSE enables faster and more sensitive one-pot testing than SHINE. a, Schematic representation of the reverse transcription, RPA, IVT and CRISPR-mediated detection processes. **b**, Amplicon accumulation in REVERSE and SHINE. The RPA reaction and LwaCas13a–crRNA were incubated at 37 °C for 0, 5, 10, 15, 20, 25 and 30 min. The resulting amplicons were analyzed through TAE-Gel electrophoresis. Arrows indicate 140 and 103 bp amplicon products for REVERSE and SHINE, respectively. **c**, Competition between reverse transcription (RT) and LwaCas13a cleavage on Orf1ab IVT RNA. Orf1ab IVT RNA, reverse transcriptase and Cas13a–crRNA were incubated at 37 °C for 5 min, following which the generated cDNA was quantified using qPCR. The levels of cDNA were normalized to the level in the 'No crRNA' group. **d**, Fluorescence profiles of REVERSE and SHINE. **e**, Sensitivity comparison between REVERSE and SHINE. Fluorescence values from one-pot testing were measured after incubating for 30 min at 42 °C. Mean ± s.d. of $n = 3$–6 technical replicates for **c**–**e**. **f**, Fluorescence values obtained by REVERSE for detecting SARS-CoV-2 clinical samples were assessed using the SpectraMax i3x at 42 °C. The black dashed lines represent the threshold, determined as three times the negative control fluorescence values for **e** and **f**.

all 85 samples, achieving a sensitivity of 100% (Fig. 2i,j). By contrast, Cas12b-WT exhibited a sensitivity of 77.6%, detecting 66 out of the 85 samples (Fig. 2i,j). LAMP alone exhibited substantial false positives and negatives (Extended Data Fig. 4c). The signal generated in the one-pot assay using Cas12b-2M did not exhibit a strong inverse correlation with the RT–qPCR Ct values for clinical sample detection (Fig. 2i). To mitigate potential cross-contamination, we incorporated dUTP and uracil-DNA *N*-glycosylase (UNG) into one-pot testing. In clinical settings, UNG is commonly preferred to enhance detection accuracy[48,49]. We observed that UNG exhibited varying degrees of interference with the one-pot testing in different clinical samples (Extended Data Fig. 5a,b). This differential inhibition likely contributed to the weak inverse correlation mentioned earlier. Taken together, these data demonstrated Cas12b-2M outperformed Cas12b-WT in one-pot testing.

Development of REVERSE assay based on Cas13a

We aimed to develop a CRISPR-based detection method without the need for a temperature-control device, making it competitive with the widely used antigen assay for in-home testing. Given that Cas13a displays stronger *trans*-cleavage activity compared to Cas12 orthologs, it suggested the potential for CRISPR detection using Cas13a even at lower than optimal temperatures[43]. One-pot detection combining RPA and LwaCas13a was developed to detect SARS-CoV-2 (ref. 40). This method, named SHINE, involves the reverse transcription of viral RNA to complementary DNA (cDNA) using the RPA reverse primer, followed by cDNA amplification using a forward primer that includes a T7 promoter sequence (Fig. 3a)[40]. The amplified DNA is then in vitro transcribed into RNA, which is subsequently recognized by LwaCas13a to trigger its *trans*-cleavage activity[40]. The sensitivity of SHINE was reported to be in the range of 100–1,000 cp µl^{-1} for nasopharyngeal swab samples, with a reaction time of 40 min at 37 °C (ref. 40).

We noticed that the RNA synthesized during in vitro transcription (IVT) shared the same sequence as the viral RNA in SHINE (Fig. 3a). We reasoned that viral RNA could also be recognized and cleaved by Cas13a, and the sequential sequence amplification could be interfered. Indeed, we found the reverse transcription and RPA process was severely compromised by Cas13a-mediated cleavage in one-pot testing (Fig. 3b,c). To diminish the interference with amplification while preserving Cas13a's *trans*-cleavage activity, we developed a new method (REVERSE). In REVERSE, cDNA was reverse transcribed

from the viral RNA using a short primer. Subsequently, amplification was carried out using a reverse primer incorporating a T7 promoter sequence. This arrangement ensured that the RNA transcribed from the DNA amplicons was reverse-complementary to the viral RNA, thereby providing sequence specificity to Cas13a-mediated cleavage (Fig. 3a). In support, the amplicon became evident within 5 min and subsequently accumulated in REVERSE, while the amplicon in SHINE was observed at 10 min and displayed minimal amplification overtime (Fig. 3b). When mixing the reverse transcription reaction and Cas13a in a single tube, and the abundance of cDNA was tracked using qPCR, the quantities of cDNA in REVERSE group were comparable to the no crispr-RNA (crRNA) control. This amounted to levels approximately ten times higher than that achieved in SHINE (Fig. 3c). Taken together, these data demonstrated that Cas13a did not interfere with the reverse transcription of the substrate in REVERSE.

We proceeded to assess the efficacy of both REVERSE and SHINE for SARS-CoV-2 detection. Notably, REVERSE was 10 min faster than SHINE to reach the maximum fluorescence value, and its signal value was 2.5 times higher than that of SHINE (Fig. 3d). For a direct comparison of the LOD between REVERSE and SHINE, both one-pot assays were conducted under identical conditions involving the same input volume, sample concentration, reaction volume and reaction times. REVERSE was able to consistently detect 1 cp μl^{-1} RNA samples from IVT, which is 100–1,000 times more sensitive than SHINE (100–1,000 cp μl^{-1}) (Fig. 3e). A similar trend was observed when using pseudo-virus of SARS-CoV-2 as the substrate (Extended Data Fig. 6a). On applying REVERSE to detect clinical samples of SARS-CoV-2, it faithfully detected all 17 SARS-CoV-2 RNA samples, particularly those with relatively high Ct values ranging from 29.1 to 35.9 (Fig. 3f).

Optimizing REVERSE for room temperature reaction

CRISPR-based detection assays typically necessitate elevated reaction temperatures ranging from 37–60 °C, whereas antigen-based detection operates at room temperature[16–19]. Despite the rapidity and sensitivity of CRISPR-based one-pot testing, the requirement for a heating device introduces higher cost and hampers its widespread use in a manner comparable to antigen tests. To assess the feasibility of REVERSE functioning at lower temperatures, we conducted REVERSE from 23 to 37 °C. REVERSE could detect pseudo-SARS-CoV-2 RNA under blue light at 23 °C within 45 min (Fig. 4a). Subsequently, we optimized REVERSE, aiming to detect viral RNA at room temperature within 30 min. To achieve this, we adjusted the concentrations of primer sets and fluorescence-quencher (Fig. 4b,c). The combination of these modifications notably accelerated the reaction rate of REVERSE, resulting in a robust signal within 30 min at 20 °C (Fig. 4d). The modified version of REVERSE, referred to as REVERSE-2, effectively detected low concentrations of pseudo-SARS-CoV-2 RNA (0.5–5 cp μl^{-1}) within 30 min at 20 °C (Extended Data Fig. 6b,c).

Detection of SARS-CoV-2 samples using REVERSE-2

To assess the applicability of REVERSE-2 for the detection of clinical SARS-CoV-2 samples at 20 °C, we tested 87 SARS-CoV-2 positive nasopharyngeal swab samples with Ct values ranging from 22.2 to 37.6, along with 20 negative samples. REVERSE-2 exhibited a sensitivity of 98.9% and a specificity of 100%, and it was capable to detect SARS-CoV-2 samples with Ct value 37.6 (corresponding to 0.5 cp μl^{-1}) within 30 min at room temperature (Fig. 4e–i). Notably, positive signals could be captured by a blue light and the camera on a smart phone, a feature that renders REVERSE-2 applicable as a straightforward self-testing kit for use at home (Fig. 4e,f).

We tested the optimized CRISPR detection mediated by Cas13a, Cas12a and Cas12b at 20 or 25 °C. While REVERSE-2 yielded detectable signals within 30 min at 20 °C, Cas12a exhibited a very weak signal at 25 °C, and Cas12b did not generate any signals (Extended Data Fig. 6d). This observation suggests that the diverse enzyme activities of Cas effectors also contribute to the detection outcome at lower than optimal temperatures.

Last, we conducted a direct comparison of the speed, LOD and specificity between REVERSE-2 and a commercially available antigen test for SARS-CoV-2, both performed at room temperature. The antigen test, with a turnaround time of 15 min, exhibited an LOD equivalent to a Ct value of 27.5 in RT–qPCR. By contrast, REVERSE-2's LOD corresponded to a Ct value of 37.3 in RT–qPCR, showcasing a sensitivity that was approximately 500–1,000 times higher than that of the antigen test (Extended Data Fig. 7a,b). Neither of the assays exhibited cross-reactivity with two other viruses, herpes simplex type 1 and human cytomegalovirus, suggesting their high specificity (Extended Data Fig. 7c,d).

Discussion

Our previous study demonstrated that targeting substrates with suboptimal PAMs accelerated one-pot testing and improved LOD and reliability[42]. Cas12a hinders the amplification process by swiftly degrading the amplicons during one-pot testing. Conversely, when using suboptimal PAM to lessen *cis*-cleavage, there is a rapid accumulation of amplicons, consequently triggering the *trans*-cleavage ability of the Cas12a (ref. 42). Although suboptimal PAMs effectively function with Cas12a, they are unsuitable for Cas12b and Cas13, which has simpler PAM or no PAM requirement (Extended Data Fig. 1). By protein engineering of PAM-interacting domains for Cas12b, a rebalancing of isothermal amplification and substrate cleavage and/or binding is achieved, thereby facilitating LAMP-mediated one-pot testing (Figs. 1 and 2 and Extended Data Figs. 2–5). This approach holds the potential for application across various Cas effectors for enhancing CRISPR-mediated nucleic acid detection capabilities.

CRISPR-based detection holds potential for point-of-care diagnosis in clinics[24,25]. For such applications, LAMP is more suitable than RPA when paired with CRISPR, owing to its single-enzyme composition, whereas RPA necessitates three enzymes, rendering LAMP a simpler choice in terms of manufacturability[50]. LAMP operates optimally at 60 °C and necessitates a thermophilic Cas protein, such as AapCas12b, for conducting nucleic acid detection within a one-pot testing[41,51]. Enhancing the sensitivity and speed of LAMP-based CRISPR detection is crucial for facilitating seamless translation into real-world usage[52]. In comparison to both Cas12b-WT and standalone LAMP, our Cas12b-2M exhibited superior performance, rendering it a competitive candidate for clinical applications (Fig. 2).

We have developed a heating-free CRISPR-based method for ultra-sensitive and rapid detecting SARS-CoV-2. In this approach, we have diminished the interference of Cas13a with the target RNA amplification process in one-pot testing (Fig. 3). This strategic design effectively capitalizes the robust *trans*-cleavage activity of Cas13a, enabling the realization of room temperature CRISPR-based detection for viral samples within a short time frame. The REVERSE-2 assay can detect viral samples with concentrations as low as 0.5 cp μl^{-1} across a range of room temperatures (20–37 °C) within a 30 min time frame (Fig. 4 and Extended Data Fig. 6). The remarkable sensitivity and accuracy exhibited by RT–qPCR set the gold standard for diagnosing various viruses, including SARS-CoV-2 (refs. 12–15). It is notable that threshold outlined in Centers for Disease Control and Prevention guidelines for qPCR falls within the range of 0.5–1 cp μl^{-1} (ref. 15). REVERSE-2 has achieved a detection sensitivity of 0.5 cp μl^{-1}, which aligns with the performance of the top-performing RT–qPCR kits. While the RT–qPCR assay demands specialized expertise, expensive infrastructure and an extended sample-to-answer duration, REVERSE-2 offers the same level of sensitivity without such complexities. The high sensitivity of REVERSE-2 is in part due to interference-free of Cas13 with amplification of the RNA substrates, as well as the streamlined design of the reverse transcription process (Fig. 4). We compared *N* gene sequences of several human coronavirus with reverse transcription primers,

https://doi.org/10.1038/s41589-023-01534-9

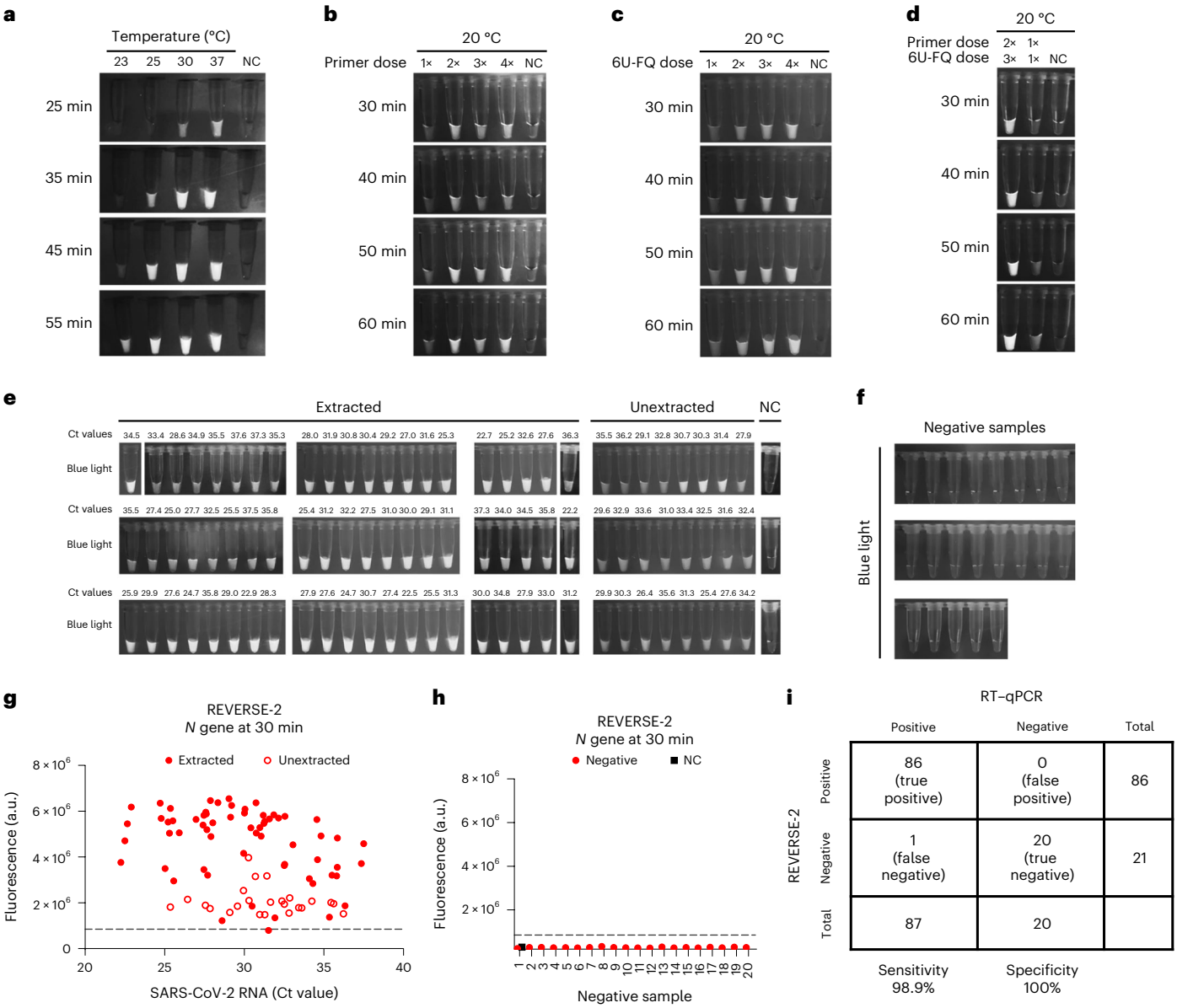


Fig. 4 | REVERSE-2 enables nucleic acids detection at room temperature. **a**, REVERSE at various temperatures. Reactions incubated at 23, 25, 30 and 37 °C for 25, 35, 45 and 55 min were analyzed using simple blue light device. The input substrates consisted of 3 cp μl^{-1} pseudo-SARS-CoV-2 RNA containing *N* gene of SARS-CoV-2. **b**–**d**, Optimizing of REVERSE at 20 °C by increasing primer dosage (**b**) and fluorescence-quencher concentration (**c**). **b**, The notation 1×, 2×, 3× and 4× represents fold changes in primer concentrations with 1× ssRNA reporter. **c**, The notation 1×, 2×, 3× and 4× represents fold changes in fluorescence-quencher concentrations with 1× primer dosage. **d**, Examination of the optimized condition. For **b**–**d**, the input substrates comprised 4 cp μl^{-1} pseudo-SARS-CoV-2 RNA containing *N* gene of SARS-CoV-2. **e**–**h**, The results using REVERSE-2 for 87 positive SARS-CoV-2 nasopharyngeal swab samples, including 63 extracted RNA and 24 unextracted samples (**e**,**g**) and 20 SARS-CoV-2 RNA negative samples (**f**,**h**). Blue light images (**e**,**f**) and fluorescence readouts (**g**,**h**) were captured at 20 °C after 30 min of incubation. The black dashed lines denote the threshold, set at three times the negative control fluorescence values for **g** and **h**. Samples with a Ct value of RT–qPCR over 38 were classified as negative sample. **i**, Concordance table comparing RT–qPCR and REVERSE-2 results for 107 samples.

amplification primers and the Cas13a–crRNA targeting sequence for SARS-CoV-2. It is evident that these sequences, especially the crRNA targeting sequence, exhibit relatively low homology, suggesting the high specificity of the REVERSE method.

Antigen-based COVID-19 kits have gained widespread popularity because of their rapid and self-testing capabilities[16–19]. While these kits offer convenience and affordability, their sensitivity is notably lower, ranging from 100 to 1,000 times less sensitive than the RT–qPCR test[16–19]. This limitation leads to a substantial number of asymptomatic and symptomatic carriers receiving false-negative results. Various self-testing kits designed for nucleic acid detection of SARS-CoV-2 have gained approval from the US Food and Drug Administration and other governmental authorities[53]. Despite their heightened sensitivity, nucleic acid detection kits' use remains much lower than that of antigen tests, in part due to their considerably elevated cost. The necessity for heating and temperature-control equipment, typically powered by USB adapters, contributes to the increased manufacturing expense of these kits. While coupling an engineered Cas13a with an electrochemical sensor has the potential to shorten reaction times to 30 min or less while enhancing sensitivity, the substantial cost associated with electrochemical sensor production and scaling up has restricted its widespread adoption[54,55]. Furthermore, a crucial application of CRISPR lies in the field detection of pathogens, wherein consistent power supplies are not always assured[37]. Notably, REVERSE-2 circumvents the

need for heating and temperature-control devices, and its sensitivity remarkably surpasses that of antigen tests while maintaining comparable detection speed (Extended Data Fig. 7).

The flexibility of CRISPR-mediated assays, coupled with their benefits of simplicity, accuracy, ultrahigh sensitivity, speed and independence from temperature control, enables diagnostics for diverse pathogen detection for field application and in-home testing. Furthermore, we believe that the enhanced LAMP-mediated CRISPR detection is poised to outperform standalone isothermal amplification in clinical settings, given its superior levels of sensitivity and specificity.

Online content

Any methods, additional references, Nature Portfolio reporting summaries, source data, extended data, supplementary information, acknowledgements, peer review information; details of author contributions and competing interests; and statements of data and code availability are available at https://doi.org/10.1038/s41589-023-01534-9.

References

1. Kuiken, T. et al. Newly discovered coronavirus as the primary cause of severe acute respiratory syndrome. *Lancet* **362**, 263–270 (2003).
2. Zhong, N. S. et al. Epidemiology and cause of severe acute respiratory syndrome (SARS) in Guangdong, People's Republic of China, in February, 2003. *Lancet* **362**, 1353–1358 (2003).
3. Zaki, A. M., van Boheemen, S., Bestebroer, T. M., Osterhaus, A. D. & Fouchier, R. A. Isolation of a novel coronavirus from a man with pneumonia in Saudi Arabia. *New Engl. J. Med.* **367**, 1814–1820 (2012).
4. Chang, S. Y., Bowman, B. H., Weiss, J. B., Garcia, R. E. & White, T. J. The origin of HIV-1 isolate HTLV-IIIB. *Nature* **363**, 466–469 (1993).
5. Dietrich, U. et al. A highly divergent HIV-2-related isolate. *Nature* **342**, 948–950 (1989).
6. Piot, P., Muyembe, J. J. & Edmunds, W. J. Ebola in west Africa: from disease outbreak to humanitarian crisis. *Lancet. Infect. Dis.* **14**, 1034–1035 (2014).
7. Petersen, L. R., Jamieson, D. J., Powers, A. M. & Honein, M. A. Zika virus. *New Engl. J. Med.* **374**, 1552–1563 (2016).
8. Hu, B., Guo, H., Zhou, P. & Shi, Z. L. Characteristics of SARS-CoV-2 and COVID-19. *Nat. Rev. Microbiol.* **19**, 141–154 (2021).
9. Zhu, N. et al. A novel coronavirus from patients with pneumonia in China, 2019. *New Engl. J. Med.* **382**, 727–733 (2020).
10. Chen, Y. et al. Emerging SARS-CoV-2 variants: why, how, and what's next? *Cell Insight* **1**, 100029 (2022).
11. Safiabadi Tali, S. H. et al. Tools and techniques for severe acute respiratory syndrome coronavirus 2 (SARS-CoV-2)/COVID-19 detection. *Clin. Microbiol. Rev.* **34**, e00228-20 (2021).
12. Osório, N. S. & Correia-Neves, M. Implication of SARS-CoV-2 evolution in the sensitivity of RT-qPCR diagnostic assays. *Lancet Infect. Dis.* **21**, 166–167 (2020).
13. Blairon, L., Piteüs, S., Beukinga, I. & Tré-Hardy, M. Development and implementation of a RT-qPCR extraction-free protocol for the detection of SARS-CoV-2 and impact on the turn-around-time. *J. Med. Virology* **93**, 2538–2542 (2021).
14. Vogels, C. B. F. et al. Analytical sensitivity and efficiency comparisons of SARS-CoV-2 RT-qPCR primer-probe sets. *Nat. Microbiol.* **5**, 1299–1305 (2020).
15. Freire-Paspuel, B. & Garcia-Bereguiain, M. A. Analytical sensitivity and clinical performance of a triplex RT-qPCR assay using CDC N1, N2, and RP targets for SARS-CoV-2 diagnosis. *Int. J. Infect. Dis.* **102**, 14–16 (2021).
16. Albert, E. et al. Field evaluation of a rapid antigen test (Panbio™ COVID-19 Ag Rapid Test Device) for COVID-19 diagnosis in primary healthcare centres. *Clin. Microbiol. Infection* **27**, 472.e7–472.e10 (2021).
17. Corman, V. M. et al. Comparison of seven commercial SARS-CoV-2 rapid point-of-care antigen tests: a single-centre laboratory evaluation study. *Lancet. Microbe* **2**, e311–e319 (2021).
18. Mak, G. C. et al. Evaluation of rapid antigen test for detection of SARS-CoV-2 virus. *J. Clin. Virol.* **129**, 104500 (2020).
19. Torres, I., Poujois, S., Albert, E., Colomina, J. & Navarro, D. Evaluation of a rapid antigen test (Panbio™ COVID-19 Ag rapid test device) for SARS-CoV-2 detection in asymptomatic close contacts of COVID-19 patients. *Clin. Microbiol. Infect.* **27**, 636.e1–636.e4 (2021).
20. Piepenburg, O., Williams, C. H., Stemple, D. L. & Armes, N. A. DNA detection using recombination proteins. *PLoS Biol.* **4**, e204 (2006).
21. Park, G. S. et al. Development of reverse transcription loop-mediated isothermal amplification assays targeting severe acute respiratory syndrome coronavirus 2 (SARS-CoV-2). *J. Mol. Diagn.* **22**, 729–735 (2020).
22. Baek, Y. H. et al. Development of a reverse transcription-loop-mediated isothermal amplification as a rapid early-detection method for novel SARS-CoV-2. *Emerg. Microbes Infect.* **9**, 998–1007 (2020).
23. Cherkaoui, D., Huang, D., Miller, B. S., Turbé, V. & McKendry, R. A. Harnessing recombinase polymerase amplification for rapid multi-gene detection of SARS-CoV-2 in resource-limited settings. *Biosens. Bioelectron.* **189**, 113328 (2021).
24. Kaminski, M. M., Abudayyeh, O. O., Gootenberg, J. S., Zhang, F. & Collins, J. J. CRISPR-based diagnostics. *Nat. Biomed. Eng.* **5**, 643–656 (2021).
25. Freije, C. A. & Sabeti, P. C. Detect and destroy: CRISPR-based technologies for the response against viruses. *Cell Host Microbe* **29**, 689–703 (2021).
26. Liu, T. Y. et al. Accelerated RNA detection using tandem CRISPR nucleases. *Nat. Chem. Biol.* **17**, 982–988 (2021).
27. Yang, L.-Z. et al. Multi-color RNA imaging with CRISPR-Cas13b systems in living cells. *Cell Insight* **1**, 100044 (2022).
28. Qiu, H.-Y., Ji, R.-J. & Zhang, Y. Current advances of CRISPR-Cas technology in cell therapy. *Cell Insight* **1**, 100067 (2022).
29. Chen, J. S. et al. CRISPR-Cas12a target binding unleashes indiscriminate single-stranded DNase activity. *Science* **360**, 436–439 (2018).
30. Li, S. Y. et al. CRISPR-Cas12a has both cis- and trans-cleavage activities on single-stranded DNA. *Cell Res.* **28**, 491–493 (2018).
31. Teng, F. et al. CDetection: CRISPR-Cas12b-based DNA detection with sub-attomolar sensitivity and single-base specificity. *Genome Biol.* **20**, 132 (2019).
32. East-Seletsky, A. et al. Two distinct RNase activities of CRISPR-C2c2 enable guide-RNA processing and RNA detection. *Nature* **538**, 270–273 (2016).
33. Fozouni, P. et al. Amplification-free detection of SARS-CoV-2 with CRISPR-Cas13a and mobile phone microscopy. *Cell* **184**, 323–333. e329 (2021).
34. Swarts, D. C. & Jinek, M. Mechanistic insights into the *cis*- and *trans*-acting DNase activities of Cas12a. *Mol. Cell* **73**, 589–600.e4 (2019).
35. East-Seletsky, A., O'Connell, M. R., Burstein, D., Knott, G. J. & Doudna, J. A. RNA targeting by functionally orthogonal type VI-A CRISPR-Cas enzymes. *Mol. Cell* **66**, 373–383.e3 (2017).
36. Gootenberg, J. S. et al. Nucleic acid detection with CRISPR-Cas13a/C2c2. *Science* **356**, 438–442 (2017).
37. Myhrvold, C. et al. Field-deployable viral diagnostics using CRISPR-Cas13. *Science* **360**, 444–448 (2018).
38. Broughton, J. P. et al. CRISPR-Cas12-based detection of SARS-CoV-2. *Nat. Biotechnol.* **38**, 870–874 (2020).
39. Patchsung, M. et al. Clinical validation of a Cas13-based assay for the detection of SARS-CoV-2 RNA. *Nat. Biomed. Eng.* **4**, 1140–1149 (2020).

40. Arizti-Sanz, J. et al. Streamlined inactivation, amplification, and Cas13-based detection of SARS-CoV-2. *Nat. Commun.* **11**, 5921 (2020).
41. Joung, J. et al. Detection of SARS-CoV-2 with SHERLOCK one-pot testing. *New Engl. J. Med.* **383**, 1492–1494 (2020).
42. Lu, S. et al. Fast and sensitive detection of SARS-CoV-2 RNA using suboptimal protospacer adjacent motifs for Cas12a. *Nat. Biomed. Eng.* **6**, 286–297 (2022).
43. Chandrasekaran, S. S. et al. Rapid detection of SARS-CoV-2 RNA in saliva via Cas13. *Nat. Biomed. Eng.* **6**, 944–956 (2022).
44. Arizti-Sanz, J. et al. Simplified Cas13-based assays for the fast identification of SARS-CoV-2 and its variants. *Nat. Biomed. Eng.* **6**, 932–943 (2022).
45. Nakauchi, M. et al. Evaluation of reverse transcription loop-mediated isothermal amplification assays for rapid diagnosis of pandemic influenza A/H1N1 2009 virus. *J. Med. Virol.* **83**, 10–15 (2011).
46. Hatano, B. et al. Mobile and accurate detection system for infection by the 2009 pandemic influenza A (H1N1) virus with a pocket-warmer reverse-transcriptase loop-mediated isothermal amplification. *J. Med. Virol.* **83**, 568–573 (2011).
47. Yang, H., Gao, P., Rajashankar, K. R. & Patel, D. J. PAM-dependent target DNA recognition and cleavage by C2c1 CRISPR-Cas endonuclease. *Cell* **167**, 1814–1828.e12 (2016).
48. Lai, M. Y. et al. Colorimetric detection of SARS-CoV-2 by uracil-DNA glycosylase (UDG) reverse transcription loop-mediated isothermal amplification (RT-LAMP). *Int. J. Infect. Dis.* **120**, 132–134 (2022).
49. Qian, C. et al. Uracil-mediated new photospacer-adjacent motif of Cas12a to realize visualized DNA detection at the single-copy level free from contamination. *Anal. Chem.* **91**, 11362–11366 (2019).
50. Minetti, C., Lacourse, E. J., Reimer, L. & Stothard, J. R. Focusing nucleic acid-based molecular diagnostics and xenomonitoring approaches for human helminthiases amenable to preventive chemotherapy. *Parasitol. Open* **2**, e16 (2016).
51. Sam, I. K. et al. TB-QUICK: CRISPR-Cas12b-assisted rapid and sensitive detection of *Mycobacterium tuberculosis*. *J. Infect.* **83**, 54–60 (2021).
52. Rödel, J. et al. Use of the Variplex™ SARS-CoV-2 RT-LAMP as a rapid molecular assay to complement RT-PCR for COVID-19 diagnosis. *J. Clin. Virol.* **132**, 104616 (2020).
53. De Felice, M., De Falco, M., Zappi, D., Antonacci, A. & Scognamiglio, V. Isothermal amplification-assisted diagnostics for COVID-19. *Biosens. Bioelectron.* **205**, 114101 (2022).
54. Yang, J. et al. Engineered LwaCas13a with enhanced collateral activity for nucleic acid detection. *Nat. Chem. Biol.* **19**, 45–54 (2022).
55. Brown, M. D. & Schoenfisch, M. H. Electrochemical nitric oxide sensors: principles of design and characterization. *Chem. Rev.* **119**, 11551–11575 (2019).

Publisher's note Springer Nature remains neutral with regard to jurisdictional claims in published maps and institutional affiliations.

Springer Nature or its licensor (e.g. a society or other partner) holds exclusive rights to this article under a publishing agreement with the author(s) or other rightsholder(s); author self-archiving of the accepted manuscript version of this article is solely governed by the terms of such publishing agreement and applicable law.

© The Author(s), under exclusive licence to Springer Nature America, Inc. 2024

Methods

Substrates preparation

The dsDNA substrates for the *Orf1ab* and *N* gene were obtained through RT–PCR (Supplementary Tables 1 and 2). The extracted SARS-CoV-2 RNA and unextracted SARS-CoV-2 samples were quantified by RT–qPCR kits (EDIAGNOSIS). Human cytomegalovirus and herpes simplex type 1 were quantified through qPCR and a plaque forming unit assay, respectively. The primers used in this study were generated by Sangon Biotech.

Preparation of crRNA and sgRNA

DNA templates that include the T7 promoter sequence were generated using PCR (Vazyme, catalog no. P505-d1) (Supplementary Tables 3 and 4). The DNA templates, along with T7 RNA polymerase and IVT buffer, were incubated at 37 °C for 2 h. Subsequently, the DNA templates were degraded using DNaseI (Promega Corporation, catalog no. M6101) and the resulting RNA products were purified using the Monarch RNA Cleanup Kit (New England Biolabs, catalog no. T2040L).

Protein expression and purification

The pET-based protein expression vector containing the protein coding sequence with a C-terminal 6× His-tag was transformed into *Escherichia. coli* strain BL21 (DE3) (WeiDibio, catalog no. EC1002). Isopropyl β-D-1-thiogalactopyranoside (Sangon Biotech, catalog no. 367-93-1) was supplemented to a final concentration of 0.5 mM once the culture density (OD_{600}) reached 0.6–0.8, and then the cultures were grown at 18 °C for an additional 16 h for AapCas12b and LwaCas13a. Subsequently, the cell lysate was collected and purified via Ni-NTA resin, with elution achieved using an elution buffer (20 mM Tris-HCl, 500 mM NaCl and 500 mM imidazole, pH 7.4). The eluted protein was collected and further purified using a gel filtration column (Superdex 200 Increase 10/300 GL), using an elution buffer consisting of 20 mM Tris-HCl and 200 mM NaCl at pH 7.4 (refs. 56,57).

Cis-cleavage

To facilitate quantification through qPCR after *cis*-cleavage, the *N* gene dsDNA substrate at concentrations ranging from 0.5 to 2.5 nM was subjected to incubation with 75 nM of AapCas12b-sgRNA RNP in a 20 µl reaction volume. The reaction mixture comprised a 1× reaction buffer (comprising 20 mM Tris-HCl, 10 mM $(NH4)_2SO_4$, 10 mM Mg_2SO_4 and 0.1% Tween 20), and the incubation was conducted at 60 °C for 1 min. Subsequently, the reactions were terminated by introducing proteinase K at 50 °C for 10 min, followed by 10 min of incubation at 95 °C to inactive proteinase K. The diluted products were quantified using qPCR. In instances where samples were destined for TAE-Gel analysis, a reaction mixture comprising 75 nM AapCas12b-sgRNA RNP and 5 nM *N* gene dsDNA substrates in a 20 µl volume was incubated at 60 °C for various time points and stopped by proteinase K. For the purpose of quantifying amplicons in one-pot testing, reactions incorporating 1 fM *N* gene dsDNA substrate were terminated by incubating the mixture at 95 °C for 10 min, followed by proteinase K digestion.

AapCas12b and LAMP-mediated one-pot testing

The LAMP-Cas12b one-pot testing was conducted in a 25 µl reaction volume with 60 nM AapCas12b RNP, 250 nM FQ ssDNA reporter, 1.4 mM of each dNTP, 8 mM $MgSO_4$, 50 mM taurine, 0.32 U $µl^{-1}$ Bst 2.0 WarmStart DNA polymerase (New England Biolabs, catalog no. M0538), 1× primer (0.2 µM F3/B3 primers, 0.4 µM Loop F/Loop B primers and 1.6 µM FIP/BIP primers). Additionally, 1× reaction buffer composed of 20 mM Tris-HCl, 10 mM $(NH4)_2SO_4$, 2 mM Mg_2SO_4 and 0.1% Tween 20 was included, along with 2 µl of substrates (Supplementary Table 5). The optimized one-pot testing designed for SARS-CoV-2 samples used 1.6 U $µl^{-1}$ Bst II plus DNA polymerase (YEASEN, catalog no. 14402ES97), 4 U $µl^{-1}$ reverse transcriptase, 0.025 U $µl^{-1}$ UNG enzyme (Biori, catalog no. E04), 40 mM KCl and 1.4 mM of each dNTP (with dTTP:dUTP ratio of 2:1). Fluorescence values were monitored using a qPCR instrument (BioRad) at 61 °C for 30 min. Alternatively, the fluorescence values were measured using the SpectraMax i3x platform following incubation in the qPCR instrument.

RPA-mediated one-pot testing using Cas12b

To prepare RPA mixture, 29.4 µl of buffer A, 1 µl of 20 µM RPA forward primer, 1 µl of 20 µM RPA reverse primer and 16.1 µl of water were added into one tube of RPA lyophilized reagent[42]. In a 30 µl reaction volume, the components included 18 µl of RPA mixture, 60 nM AapCas12b RNP, 250 nM FQ ssDNA reporter and 1 fM dsDNA substrates of *N* gene spacer 1, 2 or 3. The assay was conducted at 42 °C (Supplementary Table 6).

Reverse

A 30 µl volume for the REVERSE assay contained 50 nM LwaCas13a, 22.5 nM crRNA, 1 U $µl^{-1}$ murine RNase inhibitor (Promega Corporation, catalog no. N2111), 1.5–2.5 U $µl^{-1}$ reverse transcriptase (Thermo Fisher Scientific, catalog no. 18090010 or Lucigen, catalog no. ERT12925K), 0.05 U $µl^{-1}$ RNase H (New England Biolabs, catalog no. M0297), 2 mM of each rNTP (Sigma), 90 ng $µl^{-1}$ T7 RNA polymerase, 140 nM ssRNA reporter (FAM-UUUUUU-BHQ1, Takara Bio), 62.5 nM RPA reverse primer, 250 nM RPA forward primer, 185 nM reverse transcription primer, 11.3 µl of Buffer A, 2 µl of Buffer B (magnesium acetate) and 2 µl of RNA substrates, using RPA DNA basic kits (AMP future). In the case of REVERSE-2, the reaction used 125 nM RPA reverse primer, 500 nM RPA forward primer, 370 nM reverse transcription primer and 420 nM ssRNA reporter (FAM-UUUUUU-BHQ1, Takara Bio). Fluorescence values were measured after a 30-min incubation at either 42 or 20 °C using the SpectraMax i3x. Additionally, the assays were visualized under blue light. The clinical samples examined in this study were approved by the Wuhan Jinyintan Hospital Ethics Committee (KY-2021-01). The unextracted samples were mixed at equal ratio with lysis buffer (QuickExtract DNA extraction solution), supplemented with 250 µM tris-2-chloroethyl phosphate (Aladdin), 0.02 µg $µl^{-1}$ Chelex-100 (BioRad Laboratories) and 1 U $µl^{-1}$ RNasin Plus (Promega Corporation, catalog no. N2111), and were boiled for 10 min. The extracted samples were obtained using kits from Liferiver (Shanghai)[42].

Competition between LwaCas13a cleavage and reverse transcription

The REVERSE reaction, lacking the RPA component as well as the forward and reverse primers, was incubated at 37 °C for 5 min, followed by 95 °C for 5 min to terminate the reaction. *Orf1ab* gene IVT RNA (2 ng) and 370 nM reverse transcription primer were used. The targeting sites of the crRNAs are within the qPCR region. The resulting cDNA was subsequently quantified through qPCR using 10 µl of 2× SYBR Green mix (Vazyme, catalog no. Q111-02), 100 nM forward and reverse primers and 2 µl of the transcription products.

Antigen test

For the antigen test, 5 µl of SARS-CoV-2 samples was mixed with the buffer provided in the COVID-19 kit (Szybio), resulting in a concentration of SARS-CoV-2 equivalent to that used in REVERSE-2. This mixture was then applied onto the sample pad of a lateral flow device, and images were captured at different time points.

Reporting summary

Further information on research design is available in the Nature Portfolio Reporting Summary linked to this article.

Data availability

Source data are provided with this paper.

References

56. Shi, Y. J. et al. DNA topology regulates PAM-Cas9 interaction and DNA unwinding to enable near-PAMless cleavage by thermophilic Cas9. *Mol. Cell* **82**, 4160–4175.e6 (2022).

57. Zhang, H.-X. et al. Cas12a-based one-pot SNP detection with high accuracy. *Cell Insight* **2**, 100080 (2023).

Acknowledgements

This work is kindly supported by Key R&D Program of Hubei Province (grant nos. 2022BCA089 to H.Y. and 2022ACA005 to Y.Z.), National Key R&D Program of China (grant nos. 2019YFA0802801, 2018YFA0801401 and 2022YFF1002801), the Ministry of Agriculture and Rural Affairs of China, the Strategic Priority Research Program of CAS (grant no. XDB29010300 to X.Z.), the National Natural Science Foundation of China (grant nos. 31871345 and 32071442 to H.Y., 31972936 to Y.Z. and 31970169 to X.Z.), State Key Laboratory for Animal Disease Control and Prevention (SKLVBF202202), Medical Science Advancement Program (Basic Medical Sciences) of Wuhan University (grant no. TFJC2018004), the Fundamental Research Funds for the Central Universities (grant nos. 2042022dx0003 and 2042022kf1190), Applied Basic Frontier Program of Wuhan City (grant no. 2020020601012216 to H.Y.) and the startup funding from Wuhan University (to H.Y. and Y.Z.). We thank the core facility of Medical Research Institute at Wuhan University for their technical supports. We thank Wuhan Easy Diagnosis Biomedicine Co. for providing some reagents.

Author contributions

H.Y. conceived, designed and managed the project. X.T. and K.Z. performed most experiments with the help of T.L., M.D. and R.J. X.T. engineered the Cas12b protein and developed a room temperature REVERSE method. X.T., K.Z. and T.L. developed one-pot testing mediated by Cas12b-mutants. X.T., K.Z. and T.L. optimized conditions for detecting viral samples. Y.Z. provided conceptual advice. X.Z., X.W. and Y.H. provided samples, and Y.H. performed related experiments. X.T. and H.Y. analyzed the data. H.Y., Y.Z. and X.T. wrote the paper with inputs from the authors.

Competing interests

H.Y., Y.Z., X.T., K.Z. and T.L. have filed a patent application (no. 202311783425.X) through Wuhan University. The other authors declare no competing interests.

Additional information

Extended data is available for this paper at https://doi.org/10.1038/s41589-023-01534-9.

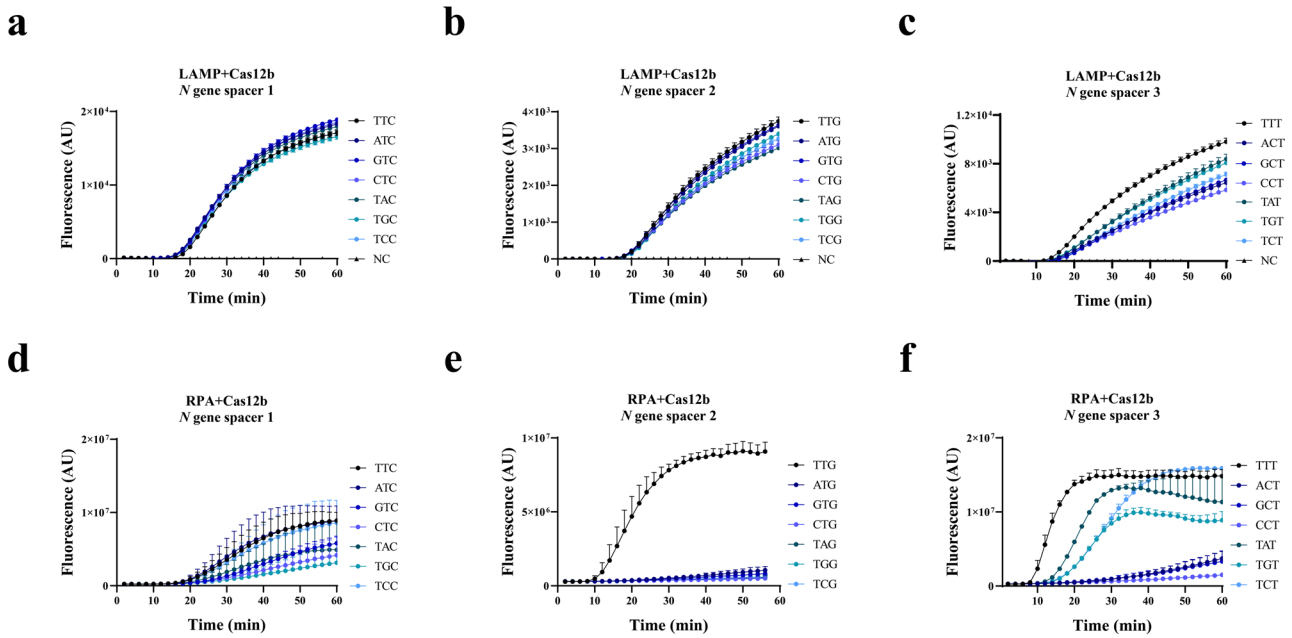
Supplementary information The online version contains supplementary material available at https://doi.org/10.1038/s41589-023-01534-9.

Correspondence and requests for materials should be addressed to Hao Yin.

Peer review information *Nature Chemical Biology* thanks the anonymous reviewer(s) for their contribution to the peer review of this work.

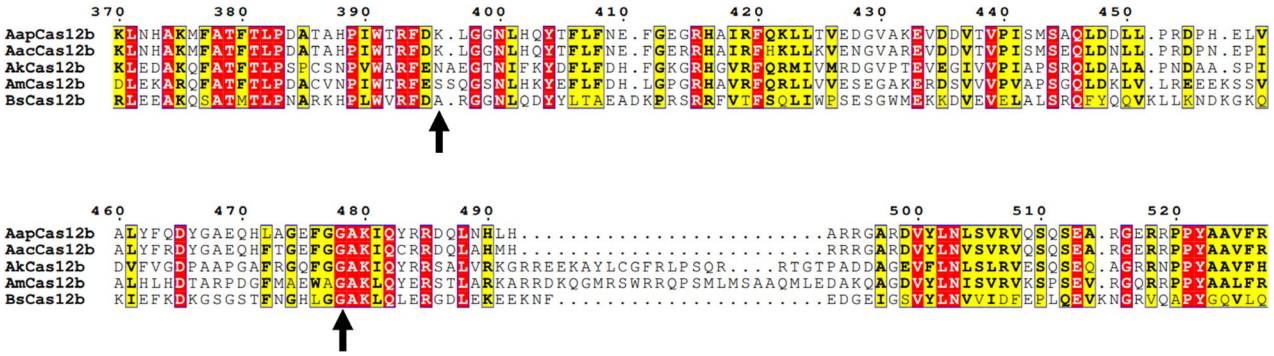
Reprints and permissions information is available at www.nature.com/reprints.

https://doi.org/10.1038/s41589-023-01534-9



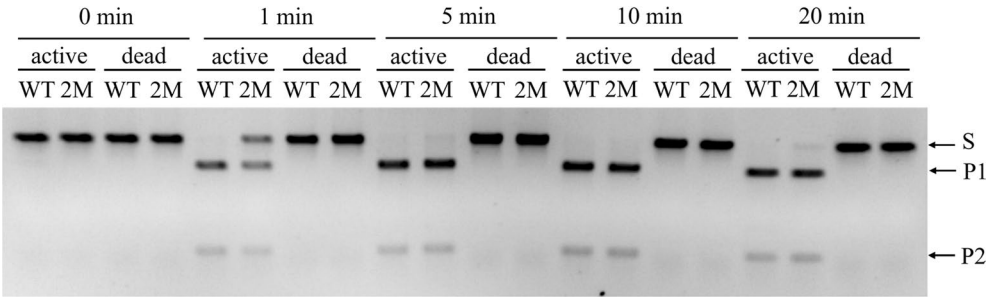
Extended Data Fig. 1 | Comparison of Cas12b-mediated one-pot testing using canonical PAM or suboptimal PAMs. (**a**–**f**) The fluorescence curves of one-pot testing using canonical PAM or suboptimal PAMs of Cas12b. For a-c, the one-pot testing was mediated by LAMP. For d-f, the one-pot testing was mediated by RPA. Mean ± s.d. for 3 technical replicates.

https://doi.org/10.1038/s41589-023-01534-9



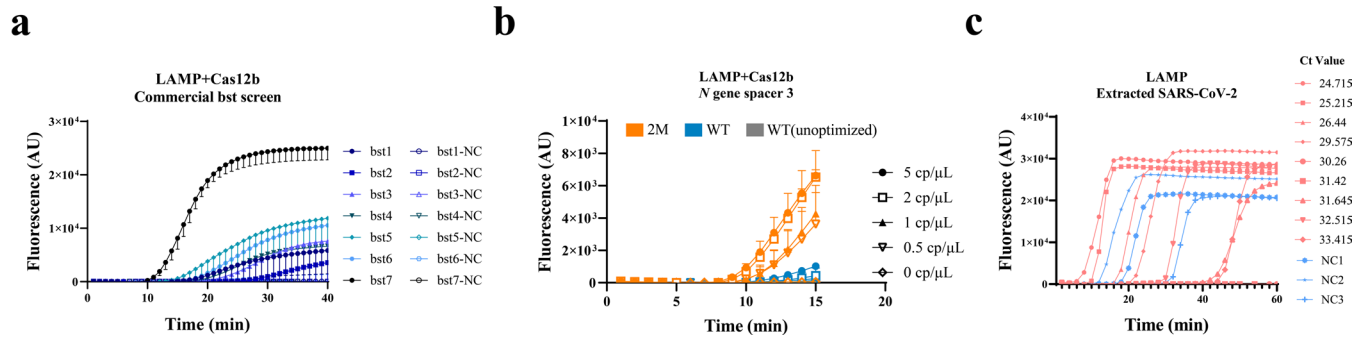
Extended Data Fig. 2 | Sequences of AapCas12b. Conservative analysis of residues 478 and 396 between Cas12b orthologs.

https://doi.org/10.1038/s41589-023-01534-9



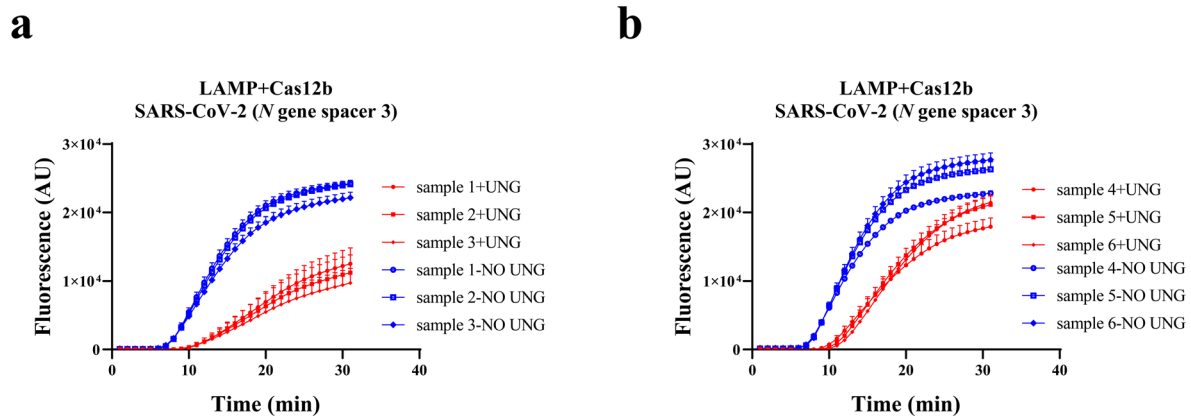
Extended Data Fig. 3 | *Cis*-cleavage of Cas12b variants. *Cis*-cleavage of Cas12b-WT, Cas12b-2M, enzymatically dead Cas12b-WT, and enzymatically dead Cas12b-2M. Enzymatically dead indicates E848A (ref. 45). Proteinase K was introduced to stop reaction at various time points. The experiment was repeated twice with similar results. S, 1241 bp substrate; P1 and P2, 927 bp product 1 and 314 bp product 2.

https://doi.org/10.1038/s41589-023-01534-9



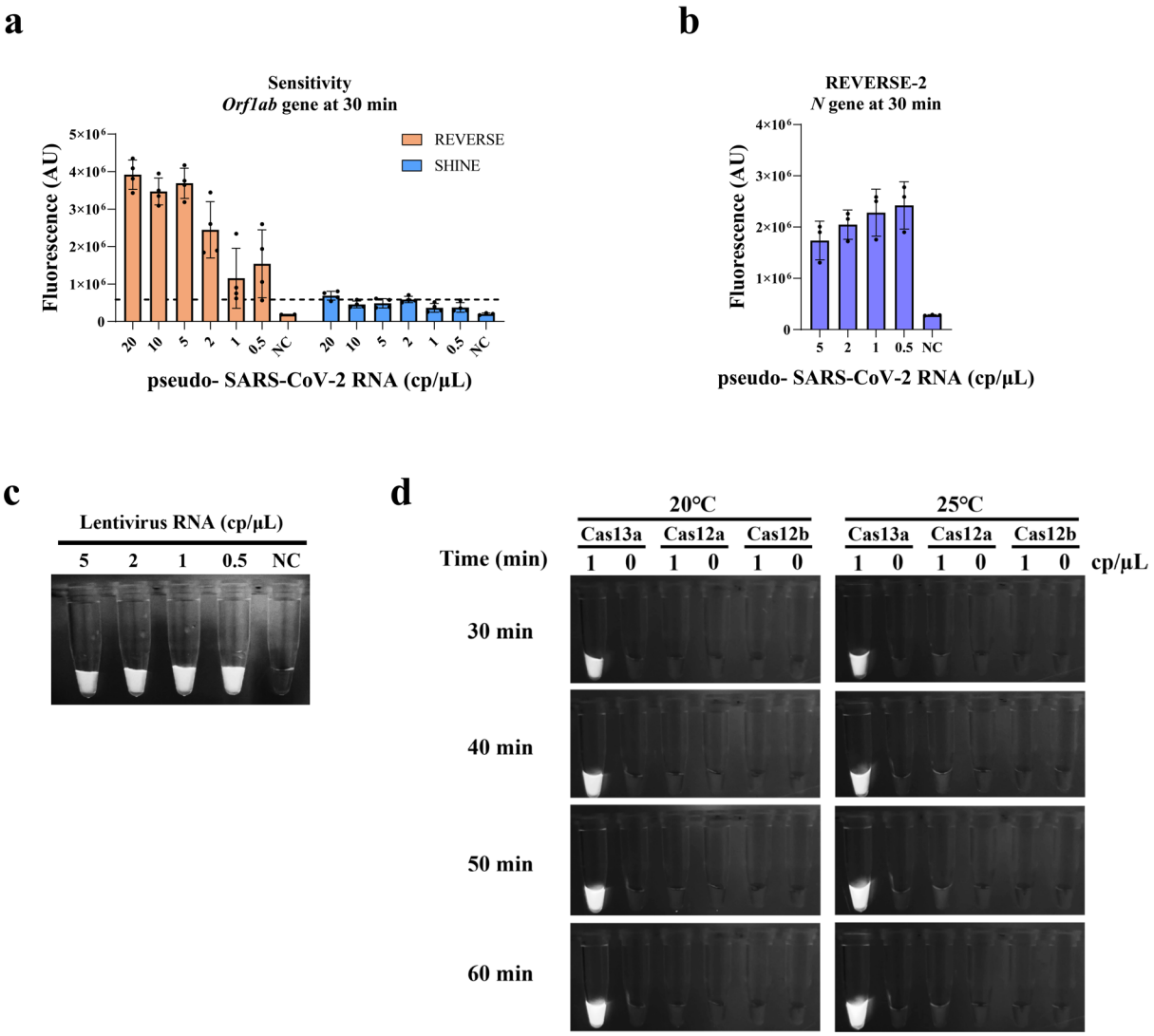
Extended Data Fig. 4 | Optimization of one-pot testing. (**a**) The performance of commercially available bst enzymes were determined in one-pot testing at 60 °C. Bst1-7 represent bst 2.0 DNA polymerase (NEB), bst 3.0 DNA polymerase (NEB), bst DNA polymerase from Vazyme, Beyotime, FAPON-BIOTECH, YEASEN and bst DNA polymerase Plus from YEASEN. (**b**) The optimized one-pot testing using Cas12b-2M or WT. 'cp/μL' indicates the copy number per microliter in one-pot testing. For a & b, mean ± s.d. for 3 technical replicates. (**c**) LAMP alone tests of SARS-CoV-2 clinical samples.

https://doi.org/10.1038/s41589-023-01534-9



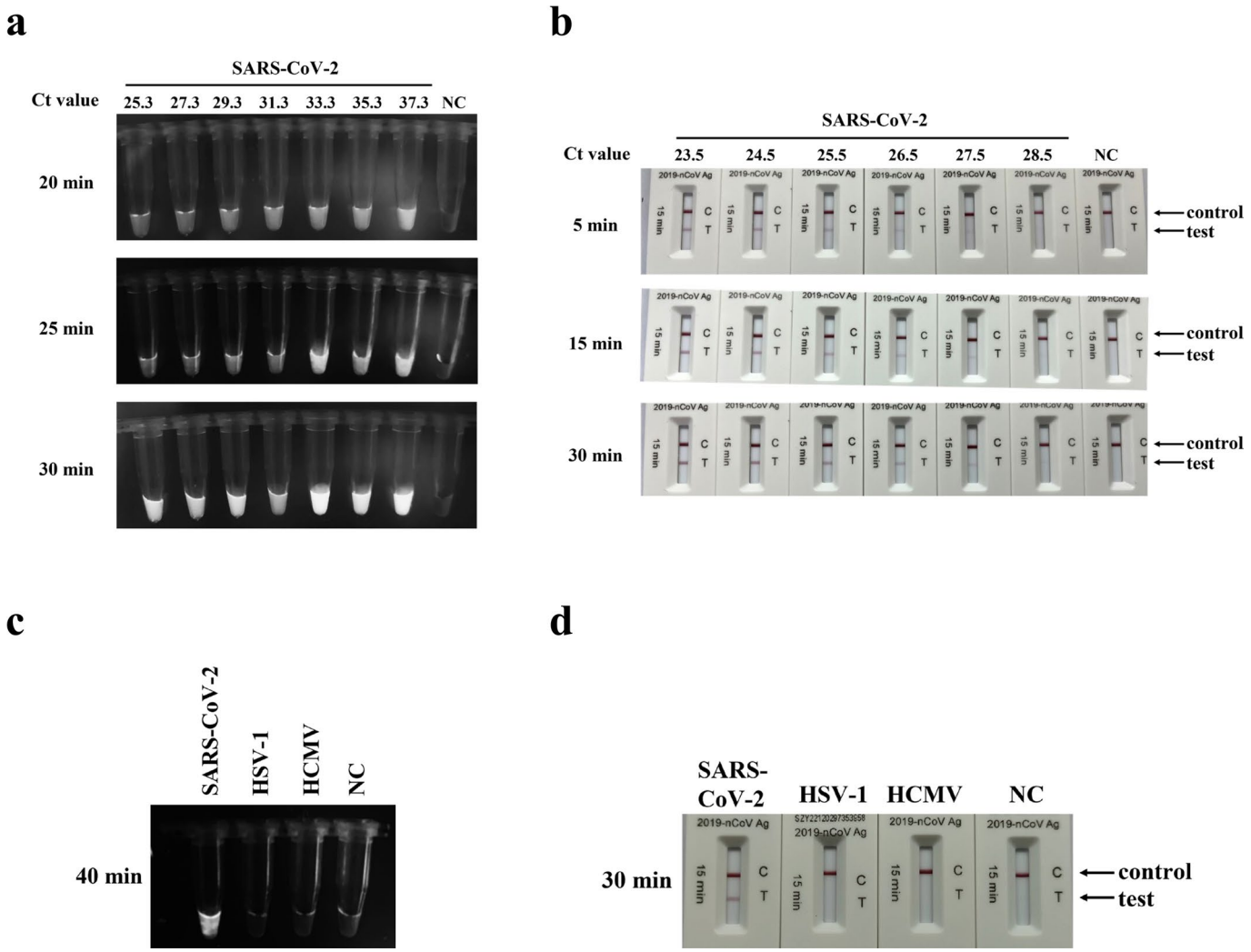
Extended Data Fig. 5 | The fluorescence curves in one-pot testing with or without UNG. (**a**-**b**) The fluorescence curves of one-pot testing with or without UNG were identified. The Ct values of clinical samples 1-6 were 23.8, 23.5, 22.6, 27.0, 33.5, and 29.0, respectively. Mean ± s.d. of n = 3 technical replicates.

https://doi.org/10.1038/s41589-023-01534-9



Extended Data Fig. 6 | Performance of REVERSE in detecting SARS-CoV-2. (**a**) Sensitivity comparison between REVERSE and SHINE. The black dotted line represents the threshold, which was determined as three times the negative control fluorescence value. (**b**, **c**) Evaluation of REVERSE-2 performance at 20 °C using a fluorescence reader (b) and blue light (c). (**d**) Comparison of Cas13a-, Cas12a- and Cas12b-mediated one-pot testing at 20 °C and 25 °C. The input substrates comprised pseudo-SARS-CoV-2 RNA of 1 cp/μL. Results were captured using blue light at 30, 40, 50, and 60 minutes. Mean ± s.d. for 4 technical replicates for a; 3 technical replicates for b.

https://doi.org/10.1038/s41589-023-01534-9



Extended Data Fig. 7 | Sensitivity and specificity comparison between REVERSE-2 and antigen test at room temperature. (**a**, **b**) Sensitivity assessment of REVERSE-2 (a) and the antigen test (b). (**c**, **d**) Determination of the specificity of REVERSE-2 and the antigen test.

nature portfolio

Corresponding author(s): Hao Yin

Last updated by author(s): Nov 21, 2023

Reporting Summary

Nature Portfolio wishes to improve the reproducibility of the work that we publish. This form provides structure for consistency and transparency in reporting. For further information on Nature Portfolio policies, see our Editorial Policies and the Editorial Policy Checklist.

Statistics

For all statistical analyses, confirm that the following items are present in the figure legend, table legend, main text, or Methods section.

n/a	Confirmed
☐	☒ The exact sample size (*n*) for each experimental group/condition, given as a discrete number and unit of measurement
☐	☒ A statement on whether measurements were taken from distinct samples or whether the same sample was measured repeatedly
☒	☐ The statistical test(s) used AND whether they are one- or two-sided *Only common tests should be described solely by name; describe more complex techniques in the Methods section.*
☒	☐ A description of all covariates tested
☒	☐ A description of any assumptions or corrections, such as tests of normality and adjustment for multiple comparisons
☐	☒ A full description of the statistical parameters including central tendency (e.g. means) or other basic estimates (e.g. regression coefficient) AND variation (e.g. standard deviation) or associated estimates of uncertainty (e.g. confidence intervals)
☒	☐ For null hypothesis testing, the test statistic (e.g. *F*, *t*, *r*) with confidence intervals, effect sizes, degrees of freedom and *P* value noted *Give P values as exact values whenever suitable.*
☒	☐ For Bayesian analysis, information on the choice of priors and Markov chain Monte Carlo settings
☒	☐ For hierarchical and complex designs, identification of the appropriate level for tests and full reporting of outcomes
☒	☐ Estimates of effect sizes (e.g. Cohen's *d*, Pearson's *r*), indicating how they were calculated

Our web collection on statistics for biologists contains articles on many of the points above.

Software and code

Policy information about availability of computer code

Data collection	No software was used.
Data analysis	No software was used.

For manuscripts utilizing custom algorithms or software that are central to the research but not yet described in published literature, software must be made available to editors and reviewers. We strongly encourage code deposition in a community repository (e.g. GitHub). See the Nature Portfolio guidelines for submitting code & software for further information.

Data

Policy information about availability of data

All manuscripts must include a data availability statement. This statement should provide the following information, where applicable:

- Accession codes, unique identifiers, or web links for publicly available datasets
- A description of any restrictions on data availability
- For clinical datasets or third party data, please ensure that the statement adheres to our policy

The data that support the findings of this study are available within this manuscript.

Human research participants

Policy information about studies involving human research participants and Sex and Gender in Research.

Reporting on sex and gender	*Use the terms sex (biological attribute) and gender (shaped by social and cultural circumstances) carefully in order to avoid confusing both terms. Indicate if findings apply to only one sex or gender; describe whether sex and gender were considered in study design whether sex and/or gender was determined based on self-reporting or assigned and methods used. Provide in the source data disaggregated sex and gender data where this information has been collected, and consent has been obtained for sharing of individual-level data; provide overall numbers in this Reporting Summary. Please state if this information has not been collected. Report sex- and gender-based analyses where performed, justify reasons for lack of sex- and gender-based analysis.*
Population characteristics	Over 100 nasopharyngeal and throat swab with SARS-CoV-2-positive or negative samples were collected.
Recruitment	Patients with SARS-CoV-2 infection. Personally identifiable information was not collected.
Ethics oversight	The clinical samples used in this study were approved by the Wuhan Jinyintan Hospital Ethics Committee

Note that full information on the approval of the study protocol must also be provided in the manuscript.

Field-specific reporting

Please select the one below that is the best fit for your research. If you are not sure, read the appropriate sections before making your selection.

☒ Life sciences ☐ Behavioural & social sciences ☐ Ecological, evolutionary & environmental sciences

For a reference copy of the document with all sections, see nature.com/documents/nr-reporting-summary-flat.pdf

Life sciences study design

All studies must disclose on these points even when the disclosure is negative.

Sample size	Over 100 samples were tested, and the experiments were performed two or more times to ensure reproducibility.
Data exclusions	No data were excluded.
Replication	Experiment was repeated twice or more with similar results, and the value of standard deviations is within expected range.
Randomization	SARS-CoV-2 samples were randomly allocated for detection.
Blinding	Blinding was not relevant to the study as the experimental procedures and data analysis did not involve subjective assessments or potential biases that could be influenced by the knowledge of sample identity.

Reporting for specific materials, systems and methods

We require information from authors about some types of materials, experimental systems and methods used in many studies. Here, indicate whether each material, system or method listed is relevant to your study. If you are not sure if a list item applies to your research, read the appropriate section before selecting a response.

Materials & experimental systems

n/a	Involved in the study
☒	☐ Antibodies
☒	☐ Eukaryotic cell lines
☒	☐ Palaeontology and archaeology
☒	☐ Animals and other organisms
☒	☐ Clinical data
☒	☐ Dual use research of concern

Methods

n/a	Involved in the study
☒	☐ ChIP-seq
☒	☐ Flow cytometry
☒	☐ MRI-based neuroimaging